Dimensional inspection of rough surfaces by optical triangulation

MANUEL F. M. COSTA
Universidade do Minho, Departamento de Fisica, P-4719 Braga Codex, Portugal. (Tel. +351 53 604327(/20); Fax. + 351 53 604339(/92))

Abstract

An optical noncontact microtopographer based on discrete active triangulation procedure which allows submicron range resolutions is described. The system is based on a simple triangulation procedure where the topographic information is obtained from the horizontal shift incurred by the bright spot created by an oblique collimated light beam on a vertical surface. A laser beam is focused on to a small, diffraction-limited spot on the surface and is made to scan over the desired region. The bright spot is perpendicularly imaged on to a linescan camera and its position obtained from the data on the individual detectors that are activated above a certain controllable intensity threshold level. The shift in the corresponding horizontal spot on the reference plane is then computed. The distance between the surface and a reference plane at each sampled point is then easily calculated. A map of the surface topography can be built and statistical surface characterization parameters calculated.

1. Introduction

While developing an optical sensor the first step to take is to define, as completely and clearly as possible the sensing task to be performed[1–5]. The following aspects need to be considered:

- the physical characteristics of the *object* of the sensing process;
- its size and boundaries of the sensed object and particular features;
- the essential and all valuable characteristics and parameters to be measured;
- process speed constraints and requirements;
- requirements and tolerance in resolution and accuracy;
- environmental constraints;
- pertinent skills of the expected operators and end users;
- operation costs; and,
- fund availability for research and development.

The kind of sensing task we are dealing with, the dimensional inspection and, specifically, the microtopographic evaluation of rough surfaces of interest to the industrial world, can be rather demanding. The variety of surfaces that need to be evaluated is very

large and hence the inspection requirements range from the 'simple' detection of discrete defects on well-*behaved* surfaces to integral topographic characterization of rough samples of little self-consistency like fabrics or organic tissues.

The range of situations makes it extremely difficult to cope with building a *universal*-type sensor which is versatile and has a wide open application field, one of the goals of major sensor designers. In fact, greater variety of surface inspection systems should be developed in view of specific sensing tasks and constraints.

Instead of trying to apply directly the existing sensors or inspection systems to a particular sensing task, it is worthwhile to analyze the possibility of rearranging the chosen system or to adapt the sensing method or strategy in view of one's particular inspection problem. In our case, research began on a request from the Textile Engineering Department of our University. Thickness and rugosity of fabrics were being measured for many years using contact gauges and *stylus*-like sensors. Deformation of sample occurs, to a smaller or deeper extent, during the inspection process depending upon the material's self-consistency and on the relief characteristic of the sample. Hence, it is desirable to develop noncontact sensors to overcome this constraint.

An optical sensor was the obvious solution. Among several techniques used on this kind of dimensional sensing optical sensor[1-16], triangulation (Fig. 1) seems to be the best solution, if not the only one, to the problem on hand.

In general, a light beam shines on a surface at a certain angle and the reflected light is collected at another. The relation between the measured quantity at the collection or observation arm is easily related to the height or vertical position of the sample.

The relation between the measured value, y', and the height, Z, is:

$$y' = M \frac{Z\sin(\eta + \theta)}{\cos\eta + (Z/f)\cot(\eta + \theta)},$$

where η and θ are incidence and observation angles, respectively, f and f', respectively, the focal lengths of the observation optics and $M = f'/f$ its magnification.

The relation between f and f' is chosen to get the best sensitivity of measure by taking into account the minimum working distance and the field of view. In order to reach
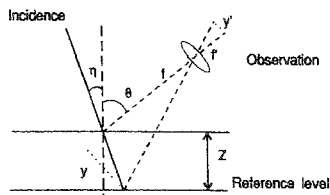

FIG. 1. The general triangulation geometry.

the best resolution, the triangulation should be large. Nevertheless, shadowing problems will become more severe.

One way of reducing the shaded areas is to make either the incidence or observation angles equal to zero (the *specular reflection geometry* ($\eta = \theta$) is, in general, of little interest for the dimensional inspection of rough surfaces).

Usually f is much larger than Z and the triangulation angle ($\eta + \theta$) is not too small ($> 5°$). Thus, eqn (1) becomes:

$$y' = MZ \sin \theta \text{ for normal incidence } (\eta = 0) \tag{2}$$

and

$$y' = MZ \tan \eta \text{ for normal observation } (\theta = 0). \tag{3}$$

From direct comparison of eqns (2) and (3) one can easily see that, for the same triangulation angle ($\eta + \theta$) the option for normal observation allows a better sensitivity than the normal incidence configuration ($S_{\theta=0}/ S_{\eta=0} = 1/\cos (\eta + \theta) > 0$).

2. Theoretical basis

After a thorough study of the physical characteristics of the particular surfaces or kind of surfaces we are interested in (remember, they will ultimately condition the sensor's performance!) we decided to use, for our dimensional inspection system, a discrete triangulation procedure with oblique incidence and normal observation[5–9].

The sample is placed on a reference surface and scanned, step by step, by an oblique laser light (definitely more suitable for use in the industrial environment) and the beam focused on to a small spot on the surface.

For each sampled point, the bright spot's position is imaged on to a linescan camera (the spot's position will always lie on the incidence plane) interfaced with a microcomputer where that spot's position will be registered. A major concern was how to locate the spot. Would it be better to consider its geometrical or the weighted centroid, and its edges? Costa and Almeida[5] observed no advantage in locating the centroids, and a spot could be located by first identifying the edge and by applying a threshold calculated as a percentage of the spot's peak intensity.

The spot shift of the reference position is calculated and the thickness, or height, and the true location of the surface point inspected at each step is computed and identified.

The three-dimensional set of coordinates is then easily established.

$$X_{n,m} = n\Delta - \delta_{n,m}/M;$$
$$Y_{n,m} = m\Phi;$$
$$Z_{n,m} = (\delta_{n,m}/M) \cotg \eta, \tag{4}$$

where η is the incidence angle, Δ, the sweep increment in the direction of the plane of incidence (X is the direction of the projection of the incidence beam on the surface plane) and Φ in the perpendicular one, M, the magnification of the observation system
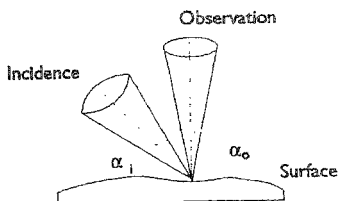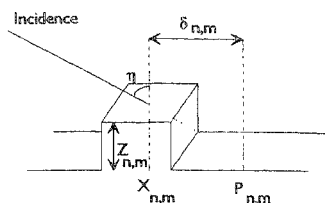
FIG. 2 The basic idea.

FIG. 3 The intersection of a light beam with a surface creates a bright spot whose later position depends on the surface height.

placed above, perpendicularly to the surface, and $\delta_{n,m}$, the spot shift (on the X direction) of a reference position $P_{n,m}$ at the scan position (X_n, Y_m).

The depth resolution (Z_{min}) attained depends upon the kind of surface to be inspected but the top value will be conditioned by the speckle effects and it will be essentially limited by the Rayleigh limit modified upon the system's particular configuration (Figs 2 and 3).

$$Z_{min} = (1/\sin \alpha_0) \, \text{cotg} \, \eta, \tag{5}$$

where α_0 is the aperture of the observation optics.

In order to get the best resolution large incidence angle should be used, the shadowing effect being the main disadvantage.

However, the realization of two inspections, the first scanning the sample using an incidence angle of η followed by an extra sampling with an opposite incidence angle of $-\eta$ will reduce this as well as the mutual reflection effect. That is important because of errors it may generate specially when non-uniform surfaces are used.

The double scanning process is illustrated in Fig. 4. One fictitious surface profile is drawn; several oblique parallel lines, representing the incident beam during the scanning process, are drawn over it. Vertical guidelines are drawn on the intersection points of the oblique lines on the surface (the bright spots viewed by the observation system). This is done for the two opposite angles η and $-\eta$ (left and right columns, respectively).

On the second row over the surface are represented the obtained height values at the 'scanning points' $(X_n = n\Delta, \Delta$ being the scanning increment), again for both the angles. The final result is a poor reproduction of the surface due to changes in height. As one can expect, on the points at levels lower than the reference one, the level at the effective position of the spot at the first inspected point appears shifted towards the light source, and to the opposite one at higher levels.

On the third row, the correct coordinates, as stated above, $(X_n = n\Delta - \delta^*_n, \delta^*_n$ being the spot shift on the surface plane $\delta^*_n = \delta_n / M)$, are used. The results are good except on the shadow zones (the possible effect of mutual reflections is ignored).

Finally, the last row shows the results of combining both η and $-\eta$ samplings. The X maximum range inspected in both the scannings is defined. Around each point of the range the first derivative is calculated (on one of the profiles, *e.g.*, the one that establishes the beginning of the X range). If it is positive, the height at that point will be that forecast with the η scanning. If it is negative, the accepted value will be the one obtained with $-\eta$. For those points when the derivative is null the mean of the η and $-\eta$ values can be calculated. It may happen that at some point of the range the first derivative is negative for the η sampling and positive for the $-\eta$, *i.e.*, both are on shadow. The results will then, in general, be incorrect. Probably the best choice will be either to ignore those on the 3-D reproduction plots or to connect directly the first good neighbours, thus averaging its heights on those points.

To calculate the height and the correct location of each evaluated surface point, the shifting of the spot on the camera plane measured in the number of pixels of the linear array needs to be converted into height value and in lateral shift on the object plane. Knowing accurately the triangulation angle (η) the lateral spot's shift at the object's plane can be easily obtained from the height value.

$$\delta_n = Z_n. \cot\eta. \tag{6}$$

On the other hand, the correspondence between the height and the pixel shift can be conveniently obtained by proceeding to the calibration of the system. A reference surface
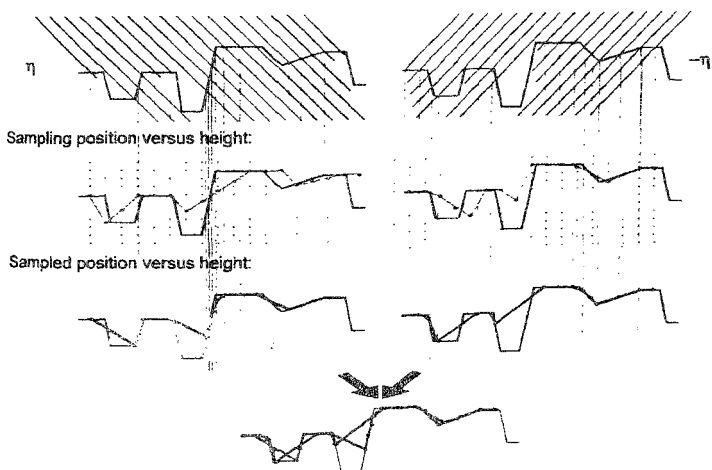

FIG. 4   Sampled position.

will be displaced vertically by accurately known increments while registering the shift of
the number of pixels of the spot. This straightforward process has the advantage of tak-
ing care of eventual misalignment or aberration in the system to some extent.

In Fig. 5, the profile of a graphite crucible is presented. Small quantity of silver pow-
der is melted in it which on removal from the crucible falls into pieces (see plot).

Two profile lines are drawn. The solid line represents the correct measured profile
and the dashed line the obtained height *versus* the lateral scanning position ($n\Delta$). As ex-
pected, in regions where the height is higher the correct profile appears shifted to the left.

3. System description

The system's configuration we chose to implement our method, being conceptually sim-
ple, is fairly versatile leading to the possibility of application to different samples and
inspection tasks.

We chose an HeNe laser at 632.8 nm as a light source despite the speckle effects on
rough surfaces. A beam steering system is used in the incidence arm of the system. The
top mirror is attached to a rotation and vertical linear displacement stage allowing easy
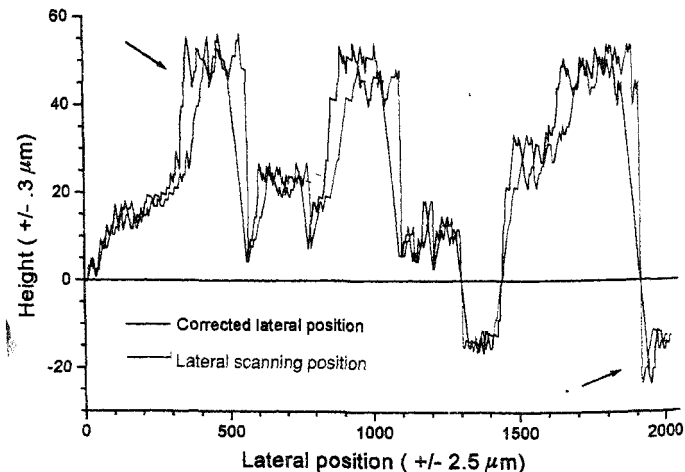incidence angle changes.

FIG. 5. The effect of the correction of the lateral inspection positions on a profile of a graphite sample with silver
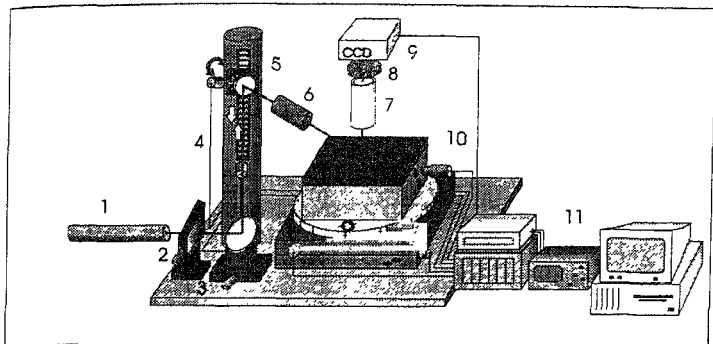impurities.

FIG. 6 The microtop 03 MFC: 1. Light source; 2: Vibration isolation stand; 3 Neutral density filter; 4. Beam steering system; 5. Incidence angle control motorized system; 6 Incidence optics; 7. Observation optics; 8. Interference filter; 9. Line scan camera; 10. Sample support and motorized positioning system; 11. Data acquisition and control system

The incidence optical system comprises a neutral density filter for optical power control and a lens system that focuses the beam on to a diffraction-limited spot of reduced dimensions.

The sample was scanned by moving it under a stationary light beam using a motorized sample positioning set-up that comprises an X, Y precision linear stage moved by two step motors allowing the sampling of points on a rectangular array separated by distances up to 1.25 μm.

A vertical movement precision stage is endowed with computer-controlled motion provided by a reliable, accurate, DC encoder with high positioning repeatability and resolution. It is used for the calibration procedure and also to keep the incidence and reception optical systems in focus over the sample.

A high-precision rotational stage provided with step motion is incorporated into the set-up in order to help the positioning of the samples and specially to allow easy change to opposite light incidence used to resolve shaded areas and mutual reflections.

A set of objectives are used to image the light spot on to a linear CCD array allowing a simple and fast acquisition process. A personal microcomputer is used to acquire and process data and to control the whole inspection process.

The dynamic range depends upon the system's configuration and application but will roughly vary between 1:300 and 1:5000. This can be increased using speckle reduction and subpixel interpolation techniques. The lateral resolution can be fairly good with high positioning accuracy obtained. The area to be expected by automatic scan is up to 25 cm^2 but can be virtually as large as desired. The measuring speed is usually not high
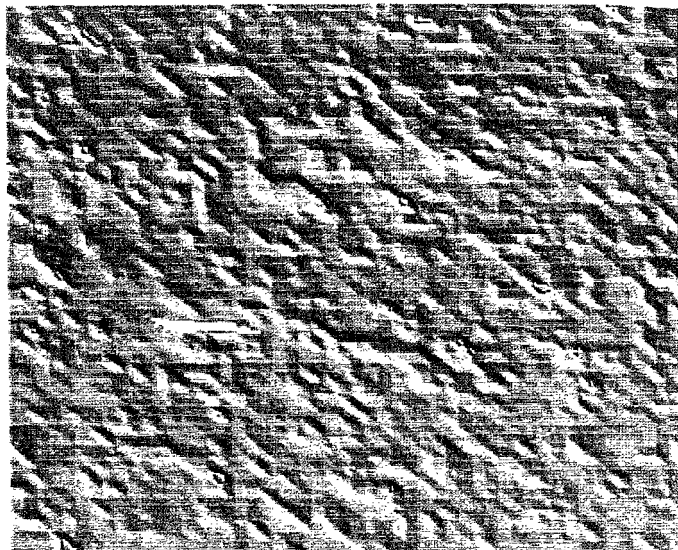
FIG 7. Relief map of red wax mold

for the kind of systems but with good components the inspection of 2000 surface points per second is possible.

3. Applications

The system has been tested in several inspection tasks on different kinds of samples: thickness measurement and relief mapping of several kinds of fabrics; polyethylene films and thin-sputtered copper, tin dioxide and silver films; roughness measurement and topographic inspection of polyethylene and wax molds, paint and graphite samples[5-9].

As an example of application we present here a representation of the micro-relief structure of a mold made of dark red wax (Fig. 7). An area of $2500 \times 2500 \ \mu m^2$ was inspected. A height resolution of 0.5 μm, for the system at this specific task, was obtained. An rms roughness of 3.4 μm was measured with a peak-to-valley of 37 μm.

4. Conclusion

Optical triangulation extensively proved its usefulness to the topographic and dimensional inspection of objects and surfaces of use or interest to industry.

A precise knowledge of the *object* of the sensing task to be performed is crucial. A closer interaction and interdisciplinary cooperation between the R&D scientists and engineers, and the manufactures should be promoted to get the best results.

References

1. BROOK, R. A.

Automatic inspection in industry today. In *Proc. Int. Conf. Industrial Inspection* (D. W. Braggins, ed.), *Proc Soc Photo-Opt Instrum. Engng*, No. 1010, pp. 2–7, 1988.

2. GROVER, C. P. (ED)

Optical testing and metrology III, *Proc. Soc. Photo-Opt. Instrum. Engng*, San Diego, No. 1332, 1990.

3. LANZL, F., PREUSS, H. AND WEIGELT, G. (EDS)

Optics in complex systems, *Proc. Soc. Photo-Opt. Instrum. Engng* Garmish Partenkirchen, No. 1319, 1990.

4. MALACARA, D. (ED)

Selected papers on optical shop metrology, SPIE Optical Engineering Press, 1990.

5. COSTA, M. F M. AND ALMEIDA, J. B.

An optical sensor for microtopographic inspection of rough surfaces, In *Proc. Int Conf. on Optics'92: From Galileo to Optoelectronics*, (P. Mazoldi, ed.), pp. 663–668, 1992, World Scientific.

6. COSTA, M. F. M. AND ALMEIDA, J. B.

System of optical non contact microtopography, *Appl Opt.*, 1993, **32**, 4860–4863.

7. COSTA, M. F. M. AND ALMEIDA, J. B.

Surface relief mapping. In *Proc. Int Conf Industrial Inspection* (D. W. Braggins, ed.), *Proc Soc. Photo-Opt. Instrum. Engng*, 1988, No. 1010, 193–199.

8. COSTA, M. F. M. AND ALMEIDA, J. B.

Surface microtopography of thin silver films. In *Proc Int. Conf Optical Testing and Metrology III*, (C. P. Grover, ed.), *Pro Soc. Photo-Opt. Instrum. Engng*, 1990, No. 1332, 544–551.

9. COSTA, M. F. M. AND ALMEIDA, J. B

Non contact optical microtopography, *Proc Soc Photo-Opt. Instrum. Engng*, 1990, No. 952–957, p. 102.

10. TAKASAKI, H.

Moire topography, *Appl. Opt.*, 1970, **9**, 1467–1472.

11. MEADOWS, D. M., JOHNSON, W. O. AND ALLEN, J. B.

Generation of surface contours by moire patterns, *Appl. Opt.*, 1970, **9**, 942–947.

12. LIM, J. S. AND CHUNG, M. S

Moire topography with color gratings, *Appl. Opt.*, 1988, **27**, 2649–2650.

13. HALIOUA, M., KRISHNAMURTHY, R. S., LIU, H. AND CHIANG, F. P.

Projection moire with moving gratings for automated 3D topography, *Appl. Opt.*, 1983, **22**, 850–855.

14. RIOUX, M.

Laser range finder based on synchronized scanners, *Appl. Opt.*, 1984, **23**, 3837–3844.

15. HAUSLER, G., HUTFLESS, J., MAUL, M. AND WEISSMANN, H.

Range sensing based on shearing interferometry, *Appl Opt.*, 1988, **27**, 4638–4644.

16. TANWAR, L. S. AND KUNZMANN, H.

An electro-optical sensor for microdisplacement measurement and control, *J. Phys. E: Sci. Instrum.*, 1984, **17**, 864–866.